ChemComm

Accepted Manuscript

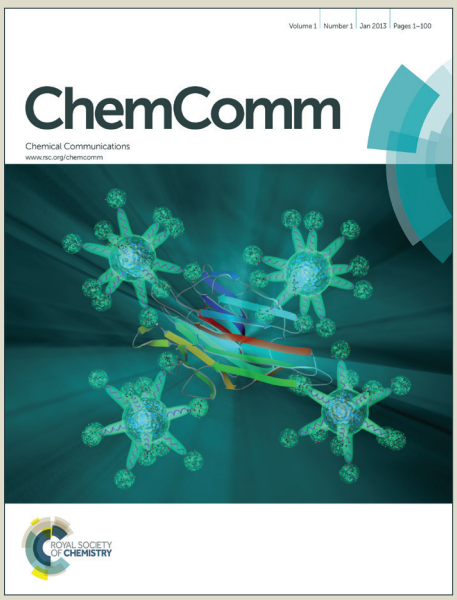

ROYAL SOCIETY OF CHEMISTRY

www.rsc.org/chemcomm

Journal Name

RSCPublishing

COMMUNICATION

Expansion of Metal-Redox Nanosynthesis: The Case Study of Iron Gallium†

Cite this: DOI: 10.1039/x0xx00000x

Alec Kirkeminde and Shenqiang Ren*

Received 00th January 2015,
Accepted 00th January 2015

DOI: 10.1039/x0xx00000x

www.rsc.org/

Metal nanoalloys have rapidly grown in importance due to their higher surface area and unique nanosized properties. Within, the metal-redox methodology is used and expanded upon utilizing FeGa as a model system. It is shown to control the stoichiometry and size of magnetic FeGa nanoalloy composites for the first time.

Metal nanoalloys have been of extraordinary interest due to their unique physical and chemical properties, such as high surface area and impressive strength.[1-4] Significant advances have been made in new methodology for the generation of these different alloy systems, which have seen use in energy-critical catalysis and nanomagnet applications.[5-9] Recently, the metal redox methodology was developed within our group that utilized zero-valent metal precursors to reduce metal salts to uniquely create nanoalloys without the use of ligands or excess reducing agents, differing it from many of the standard synthetic procedures utilized now.[10] It has been shown that the metal redox methodology can generate a vast sampling of different bimetallic alloys. However, the metals of all the created alloys exhibited vast reduction potential differences (ΔE ~ 0.20 V), allowing for the zero-valent precursor to reduce the metal salt. In order to expand the usefulness and sampling size of alloys reachable, metals with closer reduction potentials must be examined. It was observed that equilibrium of the reduction reactions could be controlled with temperature, even pushing the reaction backwards at higher temperatures. Therefore, our hypothesis is to test that high temperature could be utilized to push a non-spontaneous reaction to become spontaneous in the case of closer reduction potentials. Furthermore, being able to control shape and size will be beneficial to achieve in this nanoalloy metal-redox methodology.

The goal of this report is to expand on the versatility of the metal-redox method with three-fold objectives: 1) to show that nanoalloys of metals with very similar reduction potentials can be synthesized, 2) to demonstrate the reducing ligands could further control the stoichiometry of final nanoalloys, and 3) to utilize non-reducing ligands for the size control of final alloy nanoparticles. The FeGa system was chosen as the prototypical example alloy, as it met the requirements of both metals having close reduction potentials (Fe^{2+} = -0.44 V, Ga^{3+} = -0.53 V), and additionally, FeGa nanoalloys have never been reported in literature using the solution synthesis. Within, it is shown that nanocomposites of FeGa phases can be generated for the first time with their size being controlled with ligands, and their stoichiometry can further be controlled with the use of reducing ligands, expanding the versatility of the metal redox method.

Figure 1 displays the particles generated at different reaction temperatures, by using Iron(0) pentalcarbonyl ($Fe(CO)_5$) and Gallium(III) acetylacetonate ($Ga(acac)_3$) as the zero-valent precursor

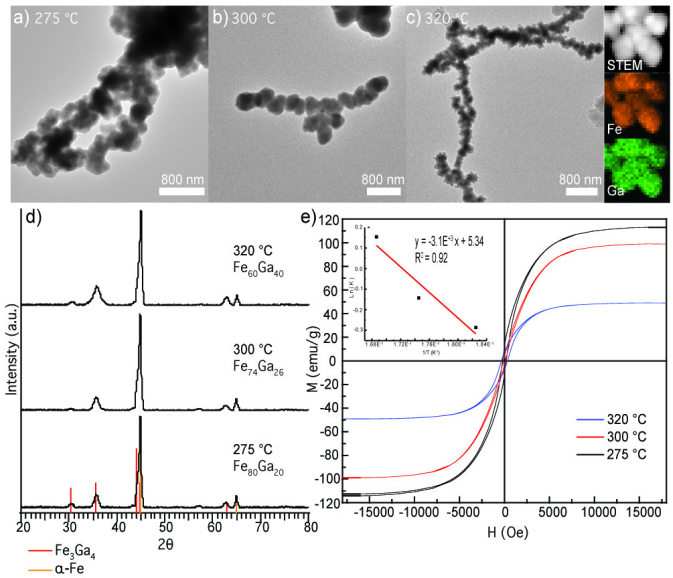

Figure 1. a-c) TEM images of nanoalloys formed at different reaction temperatures of (a) 275 °C, (b) 300 °C and (c) 320 °C. d) XRD spectrum of annealed FeGa nanocomposites, with stoichiometry of particles determined by EDS. e) M-H loop of annealed FeGa nanocomposites. Inset Van't Hoff plot.

and metal salt, respectively. It was observed that lower temperatures (< 250 °C) generate iron particles from the decomposition of $Fe(CO)_5$. At higher reaction temperatures, an increasing gallium content is observed from EDS of $Fe_{80}Ga_{20}$, $Fe_{74}Ga_{26}$ and $Fe_{60}Ga_{40}$ with respective reaction temperatures of 275 °C, 300 °C and 320 °C. The size of the standard 300 °C FeGa nanoalloy produced was 552 ± 90 nm. It is important to note that these alloys are large as there is no stabilizing ligand included to help control size. All other nanoalloys produced without ligand exhibit the same size. This higher gallium incorporation can be attributed to higher thermal energy pushing the non-spontaneous reaction backwards. In order to confirm that the FeGa nanoalloys were allowed to reach equilibrium a 4-hour reaction was conducted and displayed a $Fe_{72}Ga_{28}$ stoichiometry (Fig. S1, ESI†). This indicates that the reaction reached equilibrium at 1 hour and it is not kinetically limited. Final stoichiometry of the nanoalloys are directly related to an equilibrium constant, where a Van't Hoff plot can be constructed and fitted to a linear line, as shown in the inset of Fig. 1e (in-depth discussion for determination of equilibrium constant can be found in ESI†). Fitting a linear line generates the equation $y = -3.1x10^{+3}\ x + 5.3$, where Y is the equilibrium constant ($K=[Ga^0]/[Fe^0]$ within particles) and X = 1/T. Even with a limited thermal window for the reaction, this equation gives the ability to directly solve for the general stoichiometry of the final nanoalloys produced. Elemental mapping shows that both iron and gallium elements are present in the nanoalloys. To increase the crystallinity, the particles are annealed at 550 °C for 12 hours. The XRD spectra of annealed particles are displayed in Fig. 1d, with all showing two distinct phases, which will be deemed as FeGa based nanocomposites consisting of α-Fe and Fe_3Ga_4 phases. A higher annealing temperature of 800 °C was also used, producing the same two phases within the final nanocomposites (Fig. S2, ESI†). Within the phase diagram of FeGa, it is known that gallium is soluble in α-Fe up to ~25%, accounting for the high α-Fe diffraction intensity. The other phase matches the gallium-rich Fe_3Ga_4 phase making up the rest of the composite. Observation of this phase can be rationalized by knowing the nanoalloys start as amorphous systems, likely having distribution of metal concentrations throughout the alloy. Once annealed, these transform into the α-Fe with gallium doping and the gallium-rich Fe_3Ga_4 phase. The transmission electron microscopy (TEM) and high-resolution TEM images of post-annealed particles confirm the existence of two distinct phases within the nanocomposite and the EDS spectrum showing an iron-rich phase and gallium-rich phase, shown in Fig. S3 and S4(ESI†). To examine the effects of this different stoichiometry within the particles, magnetic hysteresis loops (M-H) were taken for the FeGa nanocomposites. The M-H loops are displayed in Fig. 1e, where the magnetic saturation (M_s) is seen drop as higher amounts of gallium within the nanocomposites, matching well with the increase of Fe_3Ga_4 phase in the XRD spectra.

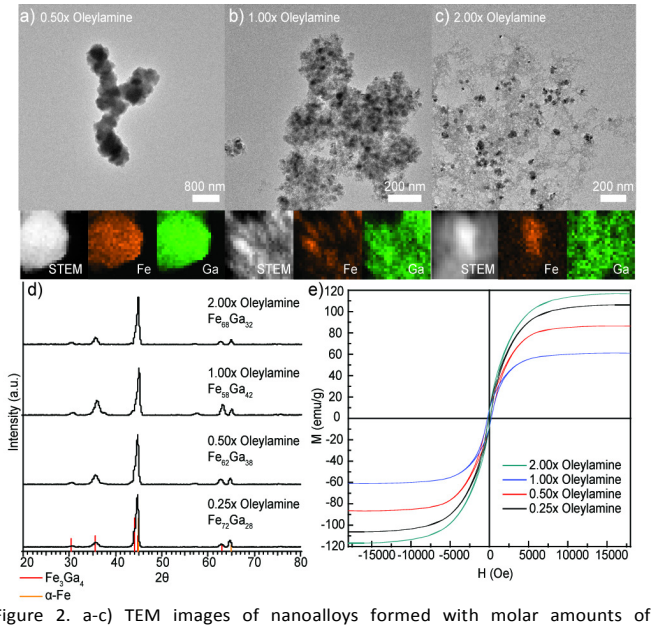

Figure 2. a-c) TEM images of nanoalloys formed with molar amounts of oleylamine to metal (a) 0.50x, (b) 1.0x and (c) 2.0x with elemental mapping of each below. d) XRD of FeGa nanocomposites after annealing with stoichiometry determined by EDS. e) M-H loops of annealed FeGa nanocomposites.

As the stoichiometry of nanoalloys in the metal-redox methodology are controlled by the equilibrium constants, and thereby temperature, final elemental ratios in the nanoalloys are limited by the boiling point of the solvent (in this case, 320 °C). In the case of the FeGa system, with the reaction only occurring at 275 °C and above, only limited stoichiometry can be achieved as seen in the above section. To overcome this limitation that arises in this system, it can be useful to make use of a ligand with inherent reducing power to help control the nanoalloy composition. Oleylamine (OA) is a well-known ligand in metal nanoparticle synthesis, as many times it also serves as the reducing agent.[11] It has been shown to be able to reduce many different metals such as Cu, Pt, Co and Fe, making it an ideal reducing agent to use in this study to help control the stoichiometry of FeGa alloys.[12] It should be noted that OA does not possess the reducing power alone to reduce $Ga(acac)_3$ used in this study, shown in Fig. S5(ESI†). Figure 2a-2c display FeGa nanoalloys and elemental mapping of particles generated using 300 °C reaction temperature with varying molar amounts of OA (i.e. the mole ratios between ligand and metal in the reaction are denoted as 0.25x, 0.5x, 1.0x, 2.0x and 4.0x). At 0.5x OA molar ratio, the particles generated look very similar to particles without OA, but an increase in Ga from $Fe_{74}Ga_{26}$ to $Fe_{62}Ga_{38}$ is observed, confirming that OA indeed can help reduce more gallium. The trend increases with a 1.0x, producing $Fe_{56}Ga_{42}$ nanoalloys, though the particles start exhibiting phase separation, as can bee seen in the elemental mapping in Fig. 2b. Upon increasing 2.0x OA, the phase separation is even more intense, as seen by the particles within the matrix. Elemental mapping confirms these separated particles are iron-rich phases. The addition of these new iron particles can be explained by having excess OA for reducing agent, as it reduces the $Fe^{2+/3+}$ ions back down to Fe^0 after it has reduced $Ga(acac)_3$. This produces final nanoalloy system having $Fe_{68}Ga_{32}$ stoichiometry, resembling initial precursor loading amounts (2:1 Fe:Ga). The back reduction of Fe ions is further confirmed by a clear supernatant after clean up, which is normally an orange solution due to iron acetylacetonate species being present. Samples having higher gallium content, such as 0.25x OA (TEM found in Fig. S6 ESI†), 0.50x and 1.0x OA ratios exhibit lager Fe_3Ga_4 peak intensities as seen in XRD spectrum in Fig. 2d. The 2.0x OA sample exhibits higher α-Fe due to the large iron particles within the nanocomposites. Magnetic saturation of the nanocomposites mimics

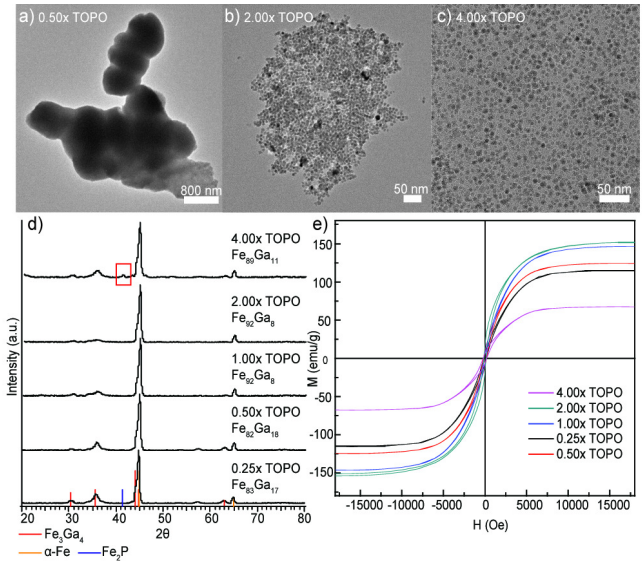

Figure 3. a-c) TEM micrographs of nanoalloys formed with molar amounts of TOPO to metal (a) 0.50x, (b) 1.0x and (c) 2.0x showing size control. d) XRD of FeGa nanocomposites after annealing with stoichiometry determined by EDS. Red box indicates Fe_2P contaminate peak at 4x TOPO concentrations. e) M-H loops of annealed FeGa nanocomposites with TOPO.

this trend, with higher iron content leading to larger saturation as shown by the M-H loops in Fig. 2e. This shows that a reducing ligand such as OA can be utilized to help control stoichiometry of the final nanocomposites, much like in standard metal nanoparticle synthesis techniques, increasing the versatility of the metal redox methodology.

To further increase the utility of the metal-redox methodology, being able to achieve size control and uniformity would be favorable over the largely uncontrolled particles produced. Trioctylphosphine oxide (TOPO) is a well-known ligand that induces the size control in many different nanoparticle syntheses, making it rational choice to use in conjunction with metal redox.[13-15] Fig. 3a-3c display TEM images of particles produced with 0.50x, 2.0x and 4.0x molar ratios of TOPO to metal, respectively. It is observed that at 0.50x TOPO ratios (Fig. 3a), the nanoalloys look similar to standard synthesis, although smaller particles are beginning to form. As the TOPO amount increases to 2.0x, nanoparticles form with a diameter of 8.9 ± 1.2 nm (higher magnification shown in Fig. S7c, ESI†), although the particles still aggregate with one another. Upon further increase of TOPO to 4.0x, the particles are completely separated from each other and shrink to a diameter of 6.2 ± 0.91 nm due to this increase in ligand concentration. Fig. 3d shows XRD of TOPO samples after annealing, as well as the stoichiometry of the final particles with varying TOPO concentrations (TEM of 0.25x and 1.0x TOPO ratios found in Fig. S7, ESI†). It can be seen that with size control comes a loss of gallium content within the final nanocomposites. The XRD confirms this low Ga with mostly α-Fe diffraction in high TOPO amount samples. Passivation and stabilization of the Fe^0 after released from the precursor by the TOPO ligand likely inhibits the reduction of the $Ga(acac)_3$. The M-H loops taken of the annealed TOPO samples shown in Fig. 3e again follow this trend of higher α-Fe exhibiting higher M_s. However, the 4.0x sample demonstrates deviation in this pattern, having lower M_s than any of the other particles. This drop is explained by the appearance of a Fe_2P peak, a nonmagnetic phase, within the XRD pattern. Phosphine doping into Fe based nanoparticles has been observed before in other iron based nanoparticle systems.[9] It is shown that the size control of metal nanoalloy synthesis could be achieved while utilizing the metal-redox methodology, making it useful for applications where the size control is required.

In conclusions, it has been shown that metal-redox methodology can be expanded to the systems with closely related reduction potentials, such as Fe and Ga, with the assistance of thermal energy. With the use of standard reducing ligands, stoichiometry of the final nanocomposites can also be tuned. Finally, size control is achieved with the use of a standard stabilizing ligand utilized in nanoparticle synthesis, making the metal redox methodology a versatile and robust nanoalloy synthesis.

Notes and references

Department of Chemistry, University of Kansas, Lawrence, KS 66045, USA. E-mail: shenqiang@ku.edu; Tel: +1-785-864-2315

Acknowledgments: This work is funded by the U.S. National Science Foundation (NSF) under Award No: NSF-CMMI-1332658.

† Electronic Supplementary Information (ESI) available: Methods and Materials, Van't Hoff plot discussion, reaction images, XRD, TEM, elemental mapping, EDS details of nanoalloys. See DOI: 10.1039/c000000x/

1. B. Poudel, Q. Hao, Y. Ma, Y. Lan, A. Minnich, B. Yu, X. Yan, D. Wang, A. Muto, D. Vashaee, X. Chen, J. Liu, M. S. Dresselhaus, G. Chen and Z. Ren, *Science*, 2008, **320**, 634.
2. T. H. Fang, W. L. Li, N. R. Tao and K. Lu, *Science*, 2011, **331**, 1587.
3. K. Lu, *Science*, 2014, **345**, 1455.
4. L. Lu, M. L. Sui and K. Lu, *Science*, 2000, **287**, 1463.
5. H. Zhang, B. Hu, L. Sun, R. Hovden, F. W. Wise, D. A. Muller and R. D. Robinson, *Nano Lett.*, 2011, **11**, 5356.
6. Y. Yu, K. Sun, Y. Tian, X. Z. Li, M. J. Kramer, D. J. Sellmyer, J. E. Shield and S. Sun, *Nano Lett.*, 2013, **13**, 4975.
7. C. Wang, H. Daimon, T. Onodera, T. Koda and S. Sun, *Angew. Chem. Int. Ed.*, 2008, **47**, 3588.
8. C. Wang, S. Peng, L.-M. Lacroix and S. Sun, *Nano Res.*, 2009, **2**, 380.
9. A. Kirkeminde and S. Ren, *Nano Lett.*, 2014, **14**, 4493.
10. A. Kirkeminde, S. Spurlin, L. Draxler-Sixta, J. Cooper and S. Ren, 2015, *Angew. Chem. Int. Ed.*, DOI: 10.1002/anie.201411460.
11. S. Mourdikoudis and L. M. Liz-Marzán, *Chem. Mater.*, 2013, **25**, 1465.
12. Y. Yu, W. Yang, X. Sun, W. Zhu, X. Z. Li, D. J. Sellmyer and S. Sun, *Nano Lett.*, 2014.
13. J. Sun, L.-W. Wang and W. E. Buhro, *J. Am. Chem. Soc.*, 2008, **130**, 7997.
14. Y. Hou, H. Kondoh, T. Ohta and S. Gao, *Appl. Surf. Sci.*, 2005, **241**, 218.
15. J. Joo, T. Yu, Y. W. Kim, H. M. Park, F. Wu, J. Z. Zhang and T. Hyeon, *J. Am. Chem. Soc.*, 2003, **125**, 6553.

TOC

A novel metal-redox methodology is utilized for the synthesis of magnetic FeGa nanoalloy for the first time.